Am J Transl Res 2023;15(3):1607-1625
www.ajtr.org /ISSN:1943-8141/AJTR0146945

Original Article

Multi-omics integrative analysis reveals the role of tumor necrosis factor superfamily member 4 in keloidal scarring

Yijun Xia[1], Youbin Wang[2], Yan Hao[1], Mengjie Shan[1], Hao Liu[2], Zhengyun Liang[1]

[1]Department of Plastic Surgery, Peking Union Medical College Hospital, Chinese Academy of Medical Sciences, Peking Union Medical College, Beijing, China; [2]Department of Plastic Surgery, Peking Union Medical College Hospital, Beijing, China

Received October 11, 2022; Accepted January 30, 2023; Epub March 15, 2023; Published March 30, 2023

Abstract: Objectives: To identify aberrantly expressed immune molecules in keloids and to explore their possible biologic significance. Methods: Immune molecules with abnormal expression were identified based on immune gene sequencing of keloids, microarray datasets and high-throughput sequencing datasets and methylation microarray datasets from the Gene Expression Omnibus (GEO) database, and real-time quantitative PCR analysis. Results: Upregulation of tumor necrosis factor superfamily member 4 (TNFSF4) in keloids was identified. Enrichment analysis found that high TNFSF4 expression was associated with immune processes, such as regulation of neutrophil chemotaxis, dendritic cell chemotaxis, and antigen processing and presentation. Single-cell RNA sequencing (scRNA) results suggested that TNFSF4 was upregulated in mesenchymal fibroblasts, which are the critical cells in skin fibrosis. This high expression of TNFSF4 enhanced cell-to-cell interactions in fibrosis-related pathways, including the fibronectin 1 (FN1) and collagen pathways. Mesenchymal fibroblasts expressing TNFSF4 significantly upregulated gene expression in extracellular matrix organization and wound healing processes. Conclusions: Our study revealed upregulation of the immune molecule TNFSF4 in keloids at the multi-omics level and its effects on intercellular crosstalk and transcriptional profiles of mesenchymal fibroblasts. Investigation of TNFSF4 as an immune checkpoint molecule may represent a new direction for keloid treatment research.

Keywords: Keloid, TNFSF4, single-cell RNA sequencing, transcriptional, methylation

Introduction

Keloid scar is a dermal fibroproliferative disorder. Abnormal excessive deposition of the extracellular matrix is its main pathologic manifestation. Keloids resemble tumors in aggressiveness, but the associated etiologic mechanisms have not been sufficiently elucidated [1-3]. Multiple elements are associated with the development of keloidal scarring, including endocrine, tension, infection, and genetics. However, there is no independent theory that explains keloid development and the accompanying clinical features. Owing to the unspecified etiology of keloids, singular symptomatic therapies like surgical excision and intra-lesion drug injection have high post-treatment recurrence rates [4].

A variety of immune molecules are gradually being recognized as essential participants in the development of keloidal scarring [5]. Skin injury is accompanied by alterations in immune cell phenotype and functions. The immune response in the pathological state disrupts the local immune homeostasis of the skin, which leads to development of fibrosis [6-8]. Increasing evidence indicates that a range of immune molecules is involved in skin fibrosis formation via effects on fibroblast proliferation, chemotaxis, and collagen synthesis. However, the mechanisms of action of dysregulated immune molecules on keloids are not fully understood [9-11].

In this study, we identified high expression of tumor necrosis factor superfamily member 4 (TNFSF4) based on sequencing of immune genes present in keloids. TNFSF4 encodes a cytokine of the tumor necrosis factor ligand family that is involved in antigen presentation and stimulates T cell activation. High expres-

sion of TNFSF4 was validated in multiple transcriptome sequencing datasets. Overexpression of TNFSF4 was found to predominantly occur in fibroblasts at a single-cell resolution; it affected intercellular crosstalk, particularly in fibrosis-related pathways. Our findings contribute to understanding the role of TNFSF4 dysregulation in keloids and provide evidence for future immunotherapy of keloids.

Materials and methods

Sequencing immune-related genes

Six young patients with keloid lesions and five healthy recipients of cosmetic surgery were randomly recruited. Samples of chest lesions collected from the patients with keloids were sequenced. The exclusion criteria were 1) patients with severe systemic disease, 2) patients with treated keloid lesions, and 3) patients younger than 18 years of age or older than 40 years of age. The Oncomine Immune Response Research Assay kit (Thermo Fisher, USA) was used to detect expression of 395 immune-related genes in the collected samples. These genes included those involved in lymphocyte regulation, cytokine signaling, lymphocyte markers, and checkpoint pathways. All experimental procedures were performed following the manufacturers' instructions.

Acquisition and pre-processing of keloid datasets

Sequenced keloid expression profiles were obtained from the Gene Expression Omnibus (GEO) database (http://www.ncbi.nlm.nih.gov/geo/); GSE44270 [12] and GSE92566 [13] were selected as test sets to assess gene expression differences between keloid and control samples. The four datasets obtained to validate target gene expression included GSE190626 [14], GSE158395 [15], GSE121618 [16], and GSE178562 [17] (**Table 1**). The "affy" package was used to perform gene name annotation; background correction was performed using the RMA algorithm to exclude the effects of non-specific factors [18]. GSE44270 and GSE92566 were combined to account for the limited sample sizes. Batch effects were removed using the "limma" package, and the effects of batch effect removal were visualized using principal component analysis (PCA) [19].

Identification of differentially expressed genes

Differentially expressed genes were screened in immune gene sequencing and GEO database expression profiles using the "limma" package, a p value less than 0.05, and a $|\log_2$ fold change$|$ greater than 1. Genes differentially expressed in the keloid lesions were revealed using volcano maps and heatmaps [19].

Methylation microarray data acquisition and processing

A matrix of genome-wide scans of methylation profiles (GSE56420) was obtained from the GEO database (keywords "methylation" and "keloid") [20]. The microarray data were quality-controlled and normalized using the "ChAMP" package, and differential analysis of the methylation sites was performed using the champ.DMP function [21].

Protein-protein and drug-protein interaction networks

Based on previous experimental data and calculations, the Search Tool for the Retrieval of Interaction Gene/Proteins (STRING) database was used to predict protein molecules that interacted with the target protein and to visualize physical and functional associations between proteins [22]. The Search Tool for Interacting Chemicals (STITCH) database was used to predict drugs that might interact with the target protein, based on drug-target relationships and binding affinities [23].

Functional enrichment analysis

Gene Ontology (GO) and Kyoto Encyclopedia of Genes and Genomes (KEGG) enrichment analysis were performed on molecules in the protein interaction network using the R package, "clusterProfiler" [24]. The combined GEO dataset was divided into two groups according to high versus low expression of TNFSF4. Gene set enrichment analysis was performed to assess functional pathways enriched in the TNFSF4 high-expression group [25].

Single-cell RNA sequencing data analysis

The keloid sample GSM5494684 and skin sample GSM5494683 were obtained from the dataset GSE181316 to observe TNFSF4

Table 1. Overview of the datasets used in this study

Dataset	Platform	Study type	Sample	
			Control	Keloid
GSE44270	Affymetrix Human Gene 1.0 ST Array	Expression profiling by array	GSM1081600 GSM1081601 GSM1081602 GSM1081603	GSM1081582 GSM1081583 GSM1081584 GSM1081585 GSM1081586 GSM1081587 GSM1081588 GSM1081589 GSM1081590
GSE92566	Affymetrix Human Genome U133 Plus 2.0 Array	Expression profiling by array	GSM2432365 GSM2432367 GSM2432370	GSM2432366 GSM2432368 GSM2432379 GSM2432371
GSE190626	Illumina NovaSeq 6000	Expression profiling by high throughput sequencing	GSM5726791 GSM5726792 GSM5726793	GSM5726788 GSM5726789 GSM5726790
GSE158395	Illumina NovaSeq 6000	Expression profiling by high throughput sequencing	GSM4798872 GSM4798873 GSM4798874 GSM4798875 GSM4798876 GSM4798877 GSM4798879 GSM4798880 GSM4798870	GSM4798878 GSM4798868 GSM4798869 GSM4798871
GSE121618	Agilent-072363 SurePrint G3 Human GE v3 8x60K Microarray 039494	Expression profiling by array	GSM3440198 GSM3440199 GSM3440200 GSM3440201 GSM3440203 GSM3440204	GSM3440194 GSM3440195 GSM3440196 GSM3440197 GSM3440202
GSE178562	Illumina HiSeq 2500	Expression profiling by high throughput sequencing	GSM5393807 GSM5393808 GSM5393815 GSM5393816	GSM5393819 GSM5393820
GSE56420	Illumina HumanMethylation450 BeadChip	Methylation profiling by genome tiling array	GSM1361173 GSM1361174 GSM1361175 GSM1361176 GSM1361177 GSM1361178	GSM1361179 GSM1361180 GSM1361181 GSM1361182 GSM1361183 GSM1361184
GSE181316	Illumina HiSeq 4000	Expression profiling by high throughput sequencing	GSM5494683	GSM5494684

GSE: Gene set ensemble; GSM: Gene set matrix.

expression patterns [26]. The "Seurat" package was used to create the objects, filtering out low-quality cells with less than 500 measured genes or with more than 5% mitochondrial genes [27]. The top 2000 high-variable genes were identified using the FindVariableFeatures function, and PCA was performed on the high-variable genes using the RunPCA function. The RunUMAP function was applied to reduce the dimensionality of the data, and the harmony function was used to remove inter-sample batch effects. Different cell types were labeled according to typical marker genes, such as fibroblasts: decorin (DCN), collagen type I alpha 2 (COL1A2), keratinocytes: keratin 1 (KRT1), keratin 14 (KRT14), macrophages: CD68 molecule (CD68), dendritic cells: fc epsilon receptor Ia (FCER1A), T cells: CD3 delta subunit of T-cell receptor complex (CD3D), smooth muscle cells: actin alpha 2 (ACTA2), melanocytes: premelanosome protein (PMEL), pericytes: regulator of G protein signaling 5 (RGS5), endothelial cells: intercellular adhesion molecule 1 (ICAM1) and lymphatic endothelial cells: lymphatic vessel endothelial hyaluronan receptor 1 (LYVE1). Cellular distribution and expression of selected genes were revealed using the DotPlot and FeaturePlot functions. The percentages of cell types expressing TNFSF4 were calculated and presented in pie charts. Genes differentially expressed between TNFSF4+ mesenchymal fibroblasts and TNFSF4- mesenchymal fibro-

Table 2. Primers and their sequences for quantitative RT-PCR analysis

Gene name	Sense primer	Antisense primer
TNFSF4	5'-ATGGTATCACATCGGTATCCTCG-3'	5'-GCCCTTCAGGGAGATGAGATAA-3'
GAPDH	5'-GGAAGCTTGTCATCAATGGAAATC-3'	5'-TGATGACCCTTTTGGCTCCC-3'

blasts were searched for using the FindMarkers function, with a *P* value less than 0.05, and a $|\log_2$ fold change| greater than 0.25 as the cut-off value.

Analysis of cell-cell communication

To characterize the effects of TNFSF4-expressing fibroblasts on intercellular communication, the fibroblast cluster was divided into a population of fibroblasts that did not express TNFSF4 and a population of TNFSF4+ fibroblasts. The CellChat package was used to infer intercellular communication involving TNFSF4+ fibroblasts and to calculate the probability of communication between all cell groups in each signaling pathway [28]. Signaling pathways with global alterations were selected for examination.

Quantitative real-time PCR assay

Tissue (100 mg) samples were extracted and ground sufficiently until no tissue mass was visible; the total RNA was then extracted and evaluated for RNA concentration and purity. Over-concentrated RNA was diluted in appropriate ratios to make a final concentration of 100-500 ng/μl. RNA was reverse transcribed into cDNA using the Servicebio® RT First Strand cDNA Synthesis Kit (G3330, Servicebio). A qPCR fluorescence kit (SYBR Green qPCR Master Mix, G3320, Servicebio) was used for quantitative analysis of TNFSF4 expression by the $2^{-\Delta\Delta CT}$ method. Each sample was assayed three times in the same run (**Table 2**).

Statistical analysis

The Mann-Whitney U test or Student's t test was used to compare continuous variables between the keloid and control groups when appropriate. R software (version 4.1.2) was used for all statistical analyses. Two-tailed *P* values < 0.05 were regarded as significant.

Results

Some tumor necrosis factor superfamily members were upregulated in expression in keloids

A flow chart of the sample processing is presented in **Figure 1**. Keloid disorder is a fibrotic disease induced by an inflammatory response that resembles autoimmune diseases characterized by the initiation of an inflammatory response that leads to tissue damage. Therefore, we sequenced immune-related genes in the keloid lesion samples, including the expression of 395 genes related to antigen presentation and processing, immune cell identification, and immune cell activation. The genes that differed significantly between keloid and normal skin samples were mainly associated with checkpoint pathways, chemokine signaling, T cell receptor (TCR) co-expression, and T cell regulation. We found upregulation of some tumor necrosis factor superfamily members (TNFSF4, TNFSF14, TNFSF18) in the keloid samples (**Figure 2A**).

Upregulation of TNFSF4 expression in keloids was validated in several datasets

While the immunogenetic sequencing results suggested that some tumor necrosis factor superfamily members were upregulated in keloids, this differential expression might not be universal. Therefore, we selected expression profile datasets from the GEO database to screen tumor necrosis factor superfamily members with stable upregulated expression. We obtained two datasets, GSE44270 and GSE92566, from the GEO database. The two datasets were combined, and batch effects were removed after normalization of the data (**Figure 2B**). The merged GEO dataset and the immune gene sequencing dataset were screened separately for differentially expressed genes, and the results were presented as heatmaps (**Figure 2C**, **2D**).

Figure 3A presents results for upregulation of TNFSF4 expression in the combined GEO dataset and the immunogenetic sequencing dataset. This elevated expression was found in GSE190626 (*P* value = 0.011), GSE158395 (*P* value = 0.003), and GSE178562 (*P* value = 2e-04) (**Figure 3B**). RT-PCR results from clinical samples revealed that TNFSF4 expression was significantly elevated in keloids, compared with normal skin tissue (**Figure 3C**).

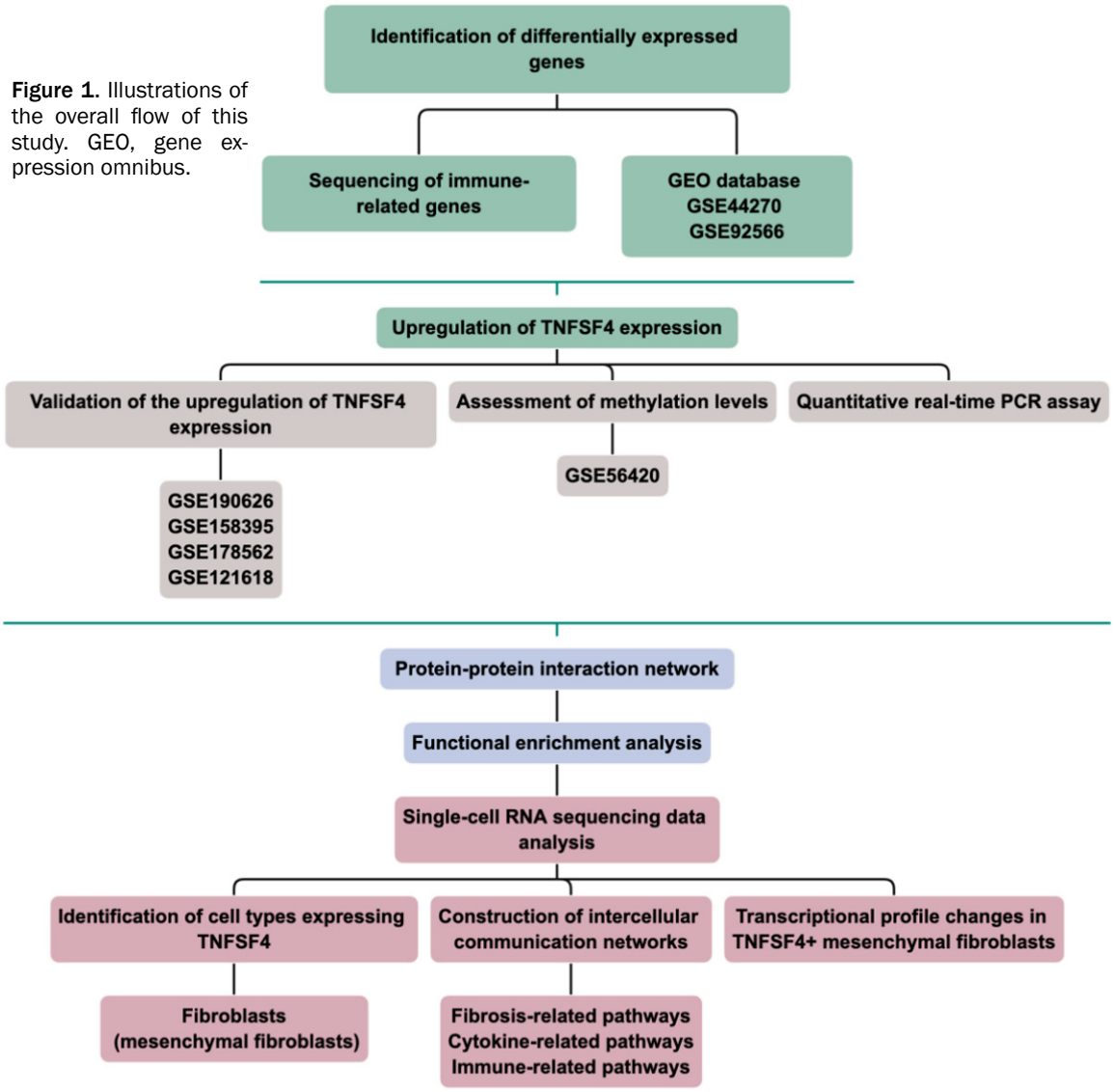

Figure 1. Illustrations of the overall flow of this study. GEO, gene expression omnibus.

To assess methylation levels of TNFSF4 in keloids, the GSE56420 dataset containing DNA methylation profiles of 485,577 cytosine phosphodiester bond guanine (CpG) was analyzed. Two differentially methylated CpG sites of TNFSF4 were detected in the body region and TSS200 (transcription start site) region. In the keloid samples, levels of methylation in the body regions of TNFSF4 were generally elevated; methylation levels in the TSS200 regions were low, overall (**Figure 3D**). Hypermethylation of the promoter suppresses gene expression and methylation of the gene body region is positively correlated with gene expression [29]. Thus, TNFSF4 methylation levels detected in the GSE56420 dataset were consistent with the TNFSF4 transcript levels mentioned above.

Enrichment analysis results indicated that TNFSF4 is involved in multiple immune processes

Considering that molecular functions are mostly accomplished via protein complex formation, protein molecules with which TNFSF4 interacted were examined in the STRING database to better understand the biologic activity of TNFSF4. A protein interaction network containing thymic stromal lymphopoietin (TSLP), CD8a molecule (CD8A), TNFSF4, TNFRSF4, TNFSF9, TNFRSF9 was constructed (**Figure 4A**). The results of functional enrichment indicated that these proteins were associated with signaling receptor activator activity, receptor ligand activity, T cell activation, and cytokine-cytokine

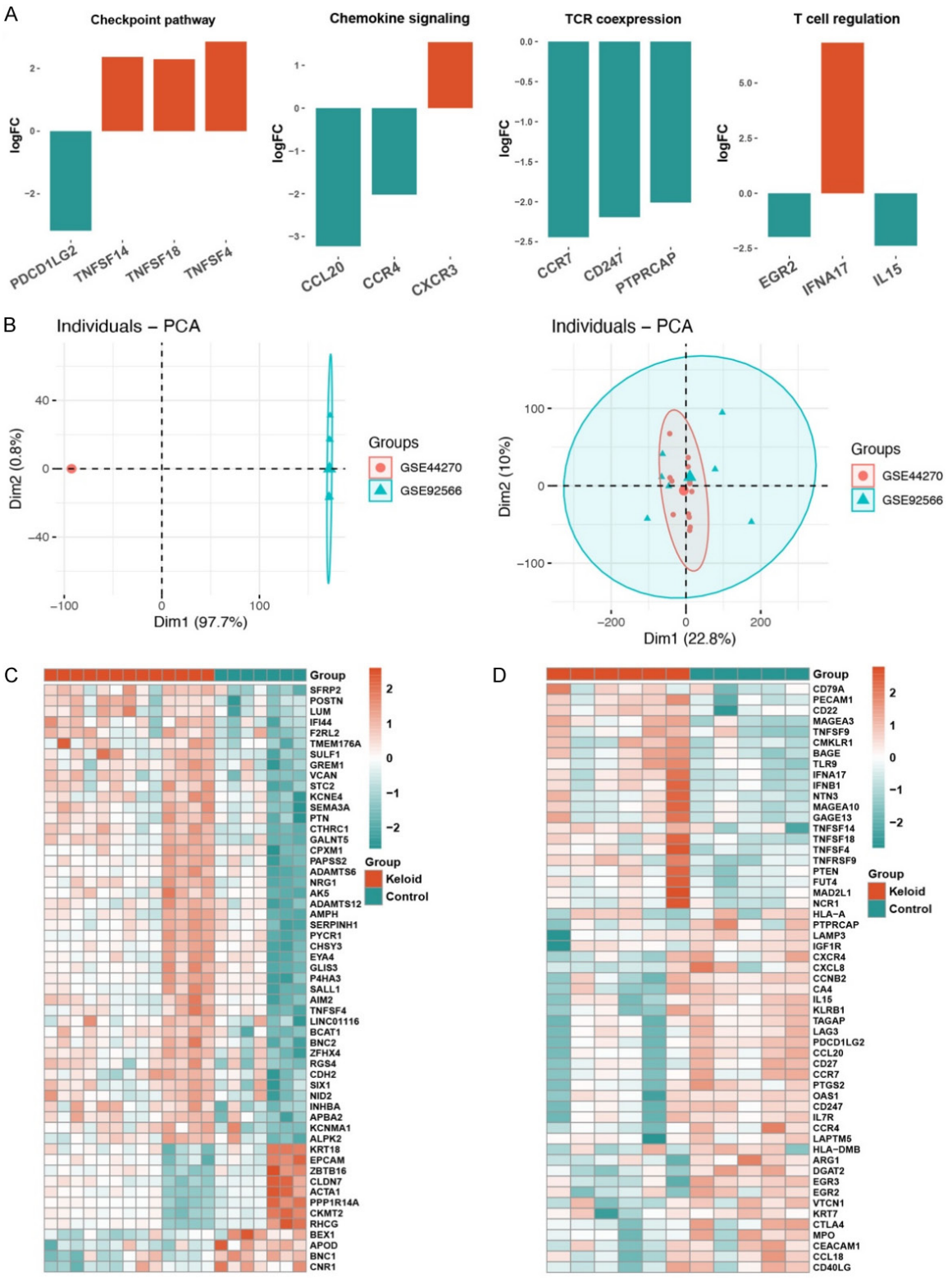

Figure 2. Identification of differentially expressed genes (DEGs). A. Sequencing of 395 immune genes, with vertical coordinates reflecting fold changes in gene expression in keloids compared to normal skins. The results suggested that significant differential genes in keloids were mainly associated with checkpoint pathways, chemokine signaling, TCR co-expression and T cell regulation. B. Batch removal effect is illustrated by principal component analysis after GSE44270 and GSE92566 were combined. The left panel shows the results of principal component analysis before batch removal, and the right panel presents the results after batch effects were removed using the ComBat

function. C. Heatmap of differentially expressed genes in the combined GEO dataset. D. Heatmap of differentially expressed genes in the sequencing of 395 immune genes. Darker red indicates a higher expression level, while deeper green means lower expression level. FC, fold change; GEO, gene expression omnibus TCR, T cell receptor.

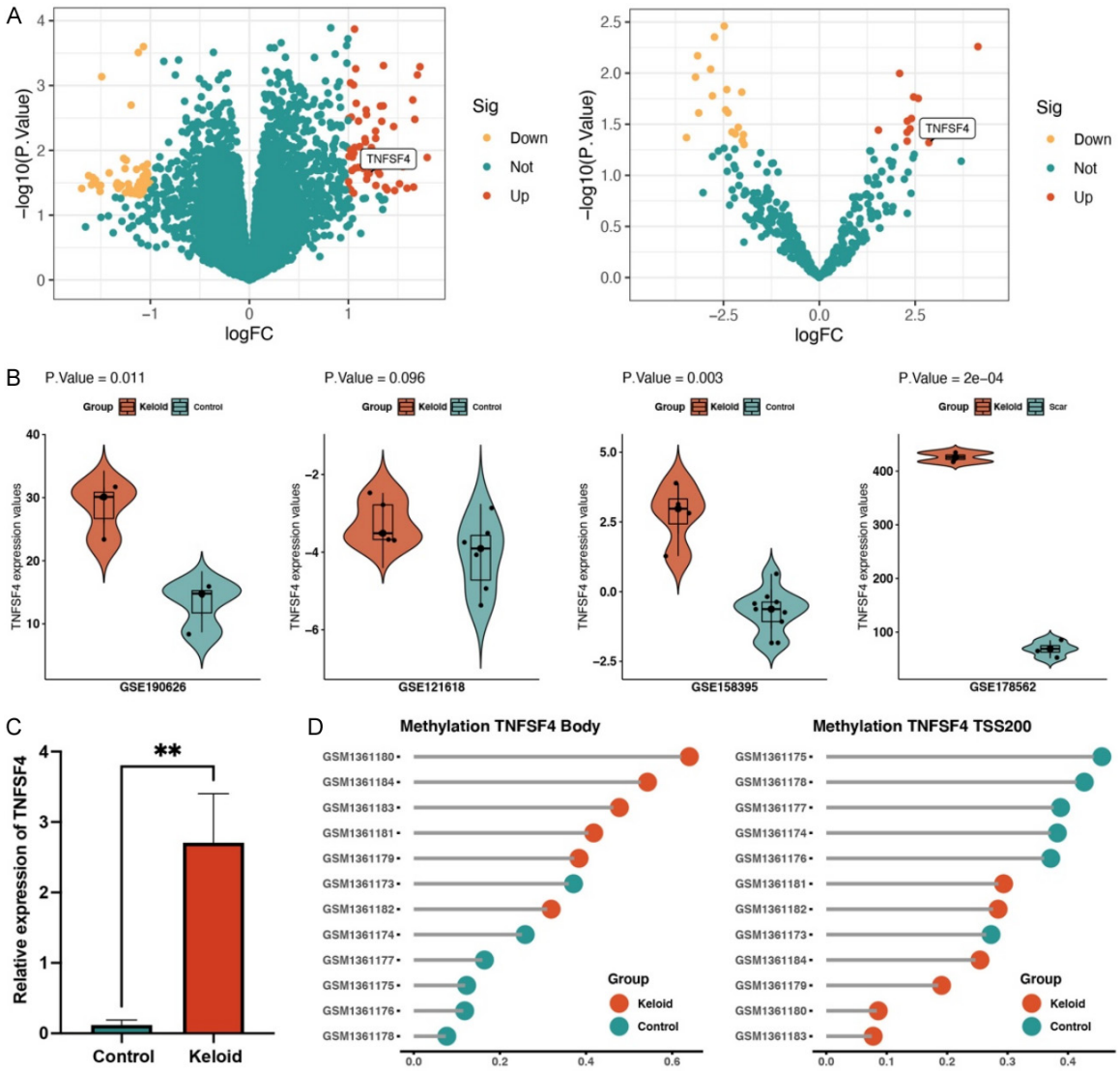

Figure 3. Identification of the target gene TNFSF4. A. Volcano map of differentially expressed genes. The GEO dataset is shown on the left, and immune sequencing is presented on the right. Yellow represents genes with low expression, green indicates genes with no significant difference in expression, and red refers to genes with high expression in keloids. TNFSF4 expression is upregulated in both datasets. B. Violin plots of elevated TNFSF4 expression validated in GSE190626 (*P*. value = 0.011), GSE158395 (*P*. value = 0.003), and GSE178562 (*P*. value = 2e-04). C. Expression levels of TNFSF4 were quantified in keloids (n = 10) and normal skin samples (n = 10) using quantitative real-time PCR analysis. D. Visualization of the methylated CpG sites of TNFSF4 located in the body region and TSS200 region, with the horizontal coordinate indicating the percentage of methylation signal intensity. CpG, cytosine-phosphodiester bond-guanine; FC, fold change; TSS, transcription start site. $^{**}P < 0.01$.

receptor interaction (**Figure 4C**, **4D**). Chitin and sulfate compounds were found to interact with TNFSF4 in the STITCH database (**Figure 4B**). Gene set enrichment analysis (**Figure 4E**) revealed that high expression of TNFSF4 in the combined GEO dataset was associated with a variety of immune processes, including regulation of neutrophil chemotaxis, dendritic cell chemotaxis, antigen processing and presentation, and the interferon-alpha response.

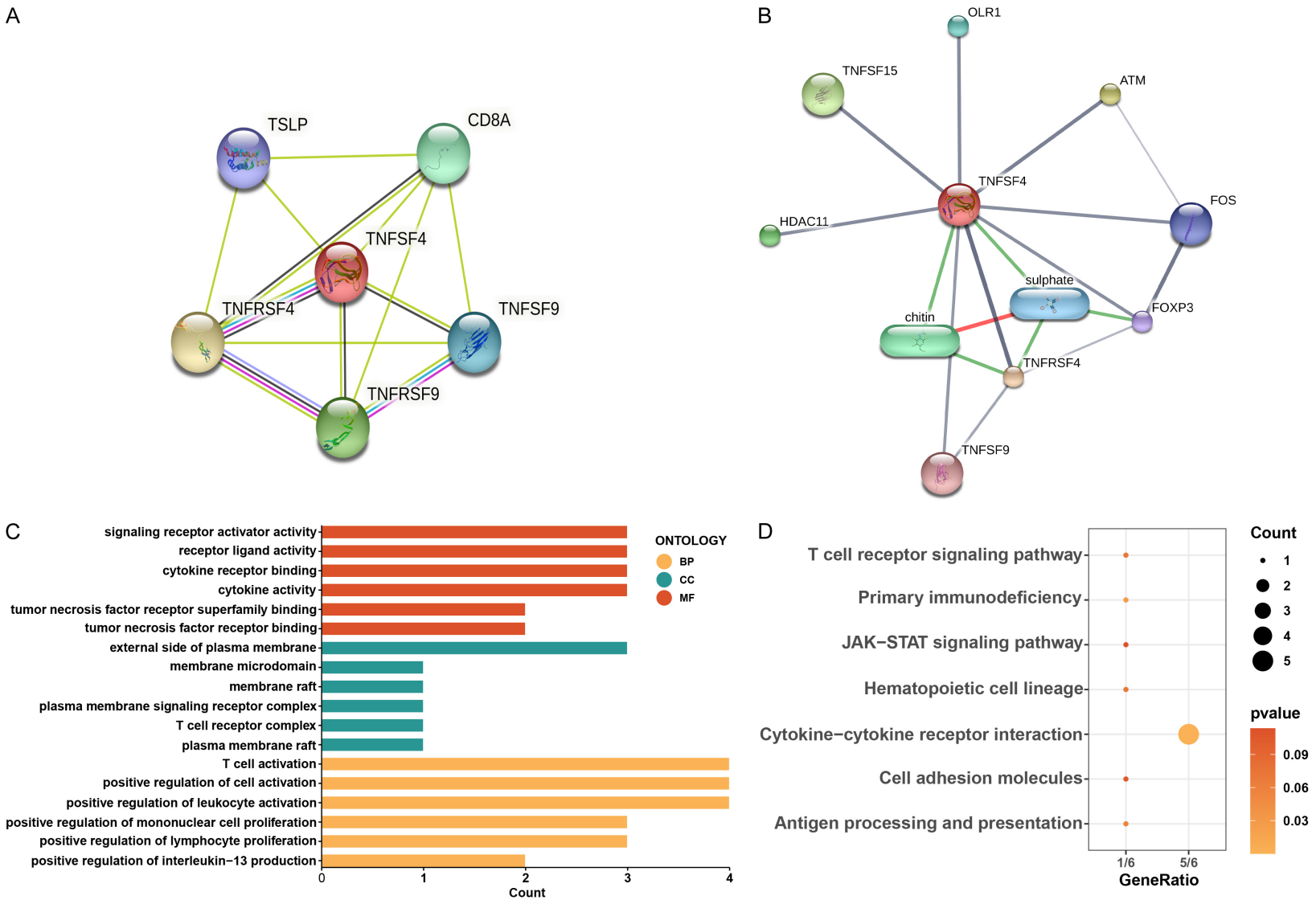
A
TSLP
CD8A
TNFSF4
TNFRSF4
TNFSF9
TNFRSF9
B
OLR1
TNFSF15
ATM
TNFSF4
FOS
HDAC11
sulphate
chitin
FOXP3
TNFRSF4
TNFSF9
C
signaling receptor activator activity
receptor ligand activity
cytokine receptor binding
cytokine activity
tumor necrosis factor receptor superfamily binding
tumor necrosis factor receptor binding
external side of plasma membrane
membrane microdomain
membrane raft
plasma membrane signaling receptor complex
T cell receptor complex
plasma membrane raft
T cell activation
positive regulation of cell activation
positive regulation of leukocyte activation
positive regulation of mononuclear cell proliferation
positive regulation of lymphocyte proliferation
positive regulation of interleukin−13 production
0
1
2
3
4
Count
ONTOLOGY
BP
CC
MF
D
T cell receptor signaling pathway
Primary immunodeficiency
JAK−STAT signaling pathway
Hematopoietic cell lineage
Cytokine−cytokine receptor interaction
Cell adhesion molecules
Antigen processing and presentation
1/6
5/6
GeneRatio
Count
1
2
3
4
5
pvalue
0.09
0.06
0.03

E

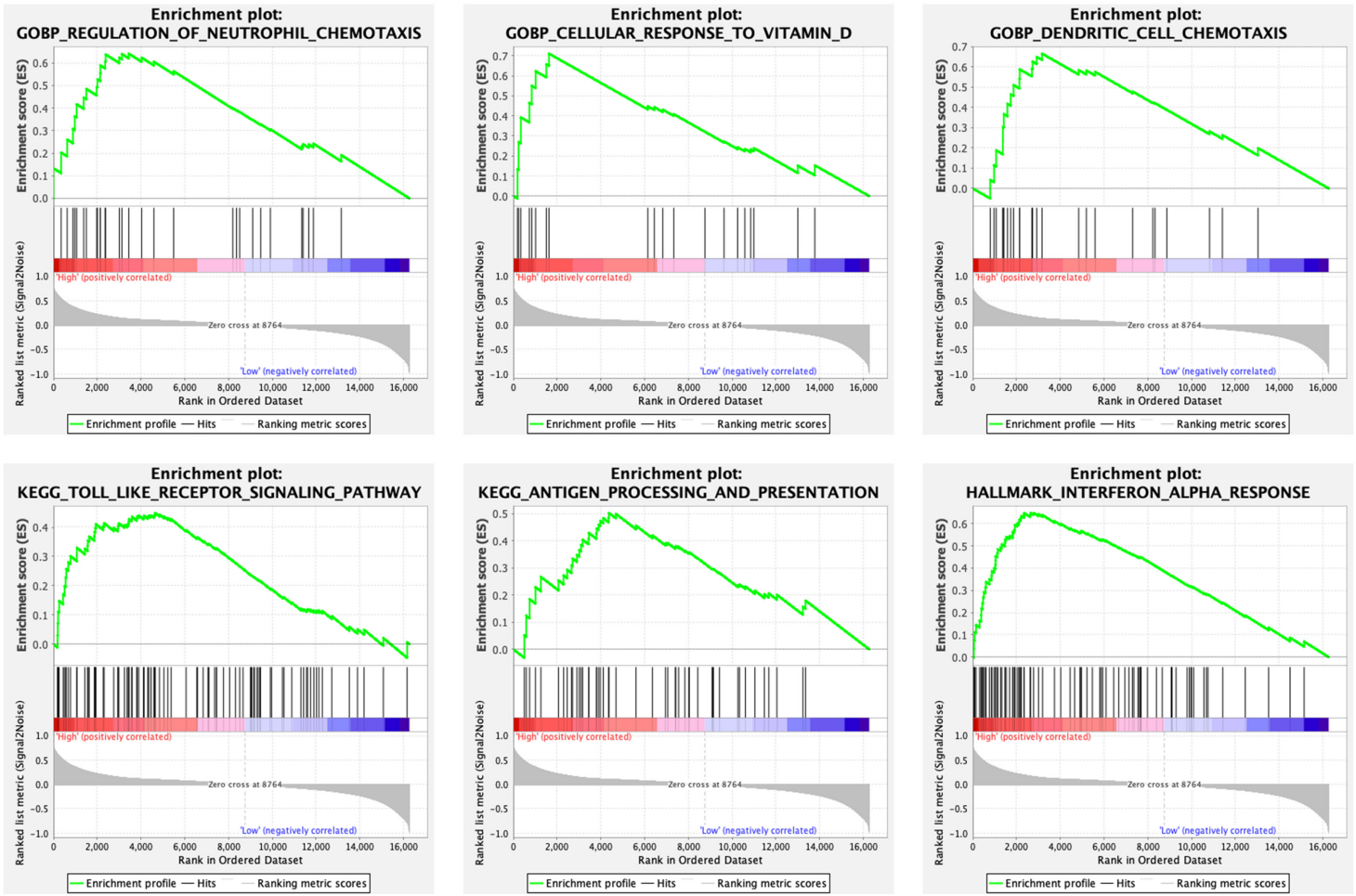

Figure 4. Functional prediction of TNFSF4. A. Visualization of protein molecules that interact with TNFSF4 in the STRING database. B. Prediction of possible compounds associating with TNFSF4 in the STITCH database. C, D. Gene ontology (GO) and KEGG pathway enrichment analysis of molecules in the protein interaction network via the R package "clusterProfiler". E. Gene set enrichment analysis of the merged GEO dataset. The expression profile data were divided into 2 groups based on TNFSF4 expression. The enriched pathways upregulated in the TNFSF4 high expression group are demonstrated.

TNFSF4 expression reshaped the intercellular communication network

We also identified cell types expressing TNFSF4 using single-cell RNA sequencing datasets to more precisely assess intercellular differences in TNFSF4 expression in keloid lesions. After correction for batch effects using the Harmony algorithm, a total of 12,330 cells were included in the downstream analysis (**Figure 5A** and Supplementary Figure 1). The unsupervised clustering algorithm identified 18 clusters that were assigned to eight cell types. Cells expressing TNFSF4 were concentrated in the fibroblast cluster (**Figure 5B**).

CellChat was then used to analyze the effect of TNFSF4 expression in fibroblasts on intercellular communication. We found that TNFSF4+ fibroblasts had a broader communication network with other clusters (**Figure 5C**), especially in fibrosis-related signaling pathways such as the fibronectin 1 (FN1), collagen, and transforming growth factor beta (TGFβ) signaling pathways (**Figure 5D**). Expression of ligands of these signaling pathways, like COL1A1, COL1A2, and FN1, was at high levels in TNFSF4+ fibroblasts (**Figure 5E**). TNFSF4+ fibroblasts are an important cellular source of the thrombospondin (THBS) pathway, and ligands of this pathway mediate cell-matrix interactions that function in wound healing, angiogenesis, and inflammatory responses [30].

Among growth factor-related signaling pathways such as the midkine (MK) pathway and the (PTN) pathway, TNFSF4+ fibroblasts increased autocrine signaling modalities, compared with TNFSF4- fibroblasts (**Figure 6**). The MK pathway and PTN pathway have been reported to promote cell growth, migration, and angiogenesis in a variety of tumors [31-33]. For epidermal growth factor (EGF) pathway, TNFSF4+ fibroblasts served as receptors increasing interaction with keratinocytes and endothelial cells and expressing higher levels of epidermal growth factor receptor (EFGR).

In immune response-related pathways, TNFSF4+ fibroblasts increased signal reception to the MIF pathway that regulates macrophage function. Expression of atypical chemokine receptor 3 (ACKR3), a receptor of this pathway, was observed in TNFSF4+ fibroblasts. TNFSF4+ fibroblasts were a key source of the c-c motif chemokine ligand (CCL) signaling pathway, and CCL2 is one of the critical chemokines that regulate migration and infiltration of monocytes and macrophages [34]. TNFSF4+ fibroblasts expressed ligands of the TWEAK signaling network. This pathway acted both in an autocrine manner and a paracrine manner from fibroblasts to keratinocytes.

TNFSF4+ mesenchymal fibroblasts possessed a pro-fibrotic transcriptional profile feature

Previous studies found that fibroblasts can be subdivided into four types, namely mesenchymal fibroblasts (MFs), pro-inflammatory fibroblasts (PFs), secretory-papillary fibroblasts (SPFs), and secretory-reticular fibroblasts (SRFs) [35]. After subdivision of fibroblasts, the results indicated that the high TNFSF4 expression was mainly clustered in MFs (**Figure 7A-D**). Prior studies found that MFs are the most variable fibroblast type and are possibly the highest-contributing cell type in keloid lesions, compared with normal scarring [36]. TNFSF4+ MFs upregulated gene expression for extracellular matrix organization, collagen binding, and wound healing processes, with a transcriptional profile characteristic of fibrosis promotion (**Figure 7F**, **7G**).

Discussion

Keloidal scarring is a refractory skin disease due to its persistent growth and aggressive nature. Because the associated pathogenic mechanisms are incompletely clarified, keloidal scarring still lacks clear molecular targets and long-lasting and effective therapies [37-39]. Considering the vital role of the immune response in keloid formation, this study aimed to identify a molecule associated with keloids based on an immune perspective and to comprehensively assess the expression and cellular distribution in a multi-omics setting. TNFSF4 and TNFRSF4 constitute a pair of co-stimulatory molecules. TNFSF4 binds to receptors on T cells and generates co-stimulatory signals that act as a facilitator of lymphocyte activation and proliferation [40]. Considering that it is an essential mechanism in tumor immune checkpoint blockade therapy and immune tolerance, identification of aberrant expression of TNFSF4 may provide a new direction for future research on keloid lesions.

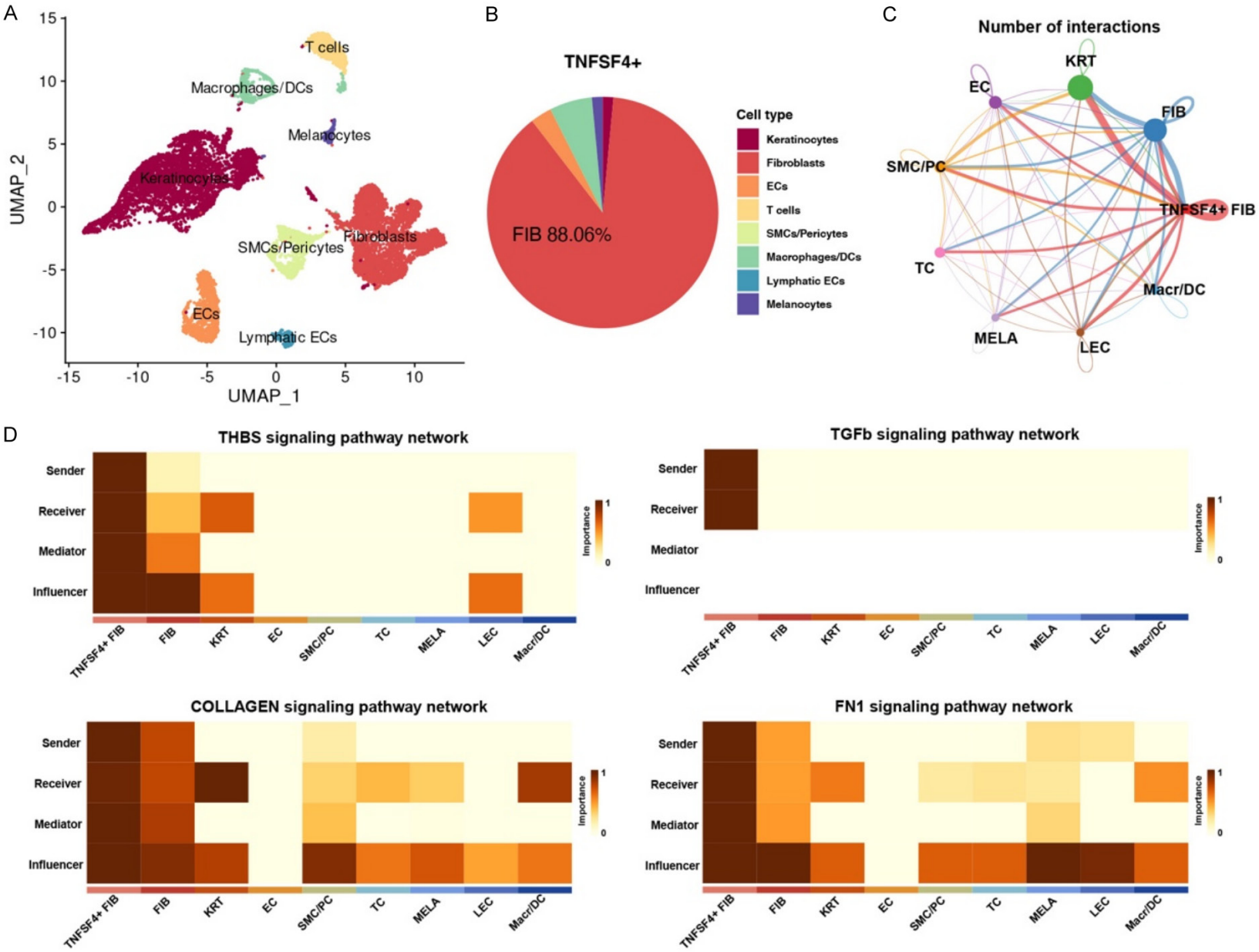
A
T cells
Macrophages/DCs
Melanocytes
Keratinocytes
Fibroblasts
SMCs/Pericytes
ECs
Lymphatic ECs
UMAP_2
UMAP_1
B
TNFSF4+
FIB 88.06%
Cell type
Keratinocytes
Fibroblasts
ECs
T cells
SMCs/Pericytes
Macrophages/DCs
Lymphatic ECs
Melanocytes
C
Number of interactions
KRT
EC
FIB
SMC/PC
TNFSF4+ FIB
TC
Macr/DC
MELA
LEC
D
THBS signaling pathway network
TGFb signaling pathway network
COLLAGEN signaling pathway network
FN1 signaling pathway network
Sender
Receiver
Mediator
Influencer
Importance
TNFSF4+ FIB
FIB
KRT
EC
SMC/PC
TC
MELA
LEC
Macr/DC

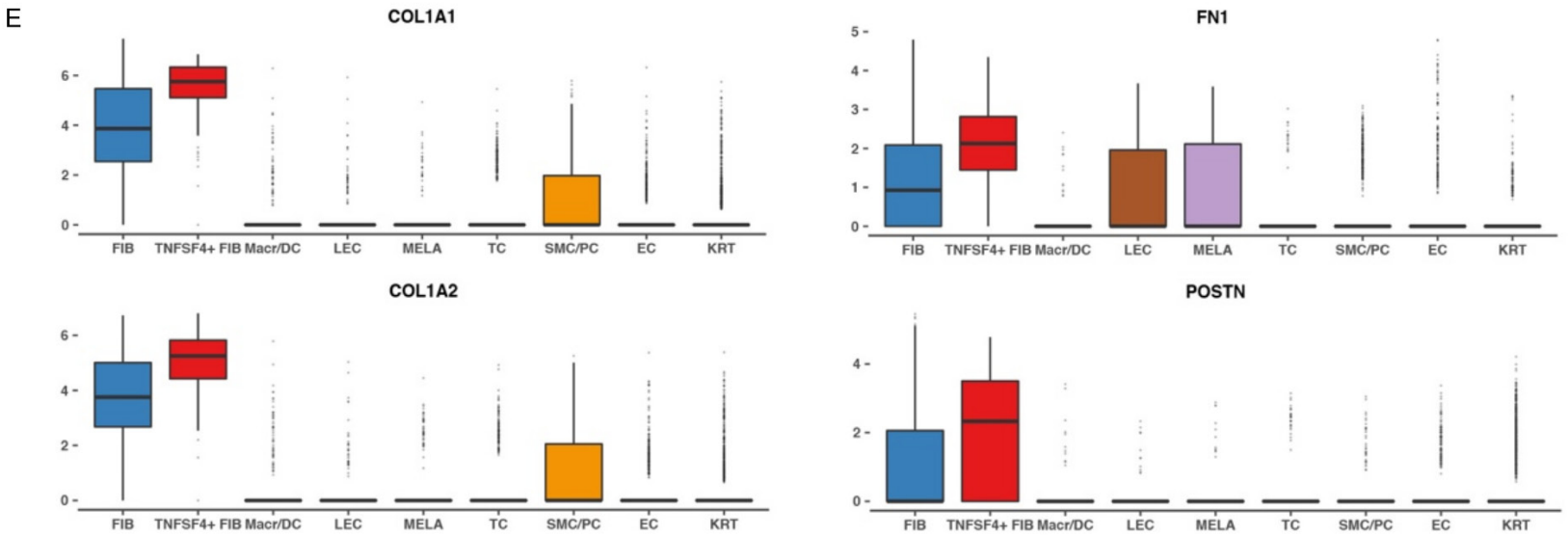

Figure 5. Cellular crosstalk in keloids. A. Eight cell types were identified after descending clustering of single-cell sequencing datasets. B. Pie chart showing the proportion of cell types expressing TNFSF4, with fibroblasts predominating. C. The number of interactions between cells. Fibroblasts expressing TNFSF4 communicate more intensively with other cells. D. Heat map showing the relative importance of each cell group based on the calculated four network centrality of THBS (thrombospondin), TGFβ (transforming growth factor beta), FN1 (fibronectin 1), and collagen signaling. E. Bar charts demonstrating the expression patterns of COL1A1, COL1A2, FN1, and POSTN. FIB, fibroblast; EC, endothelial cell; KRT, keratinocyte; MELA, melanocyte; PC, pericyte; SMC, smooth muscle cell; DC, dendritic cell; TC, T cell; Macr, macrophage.

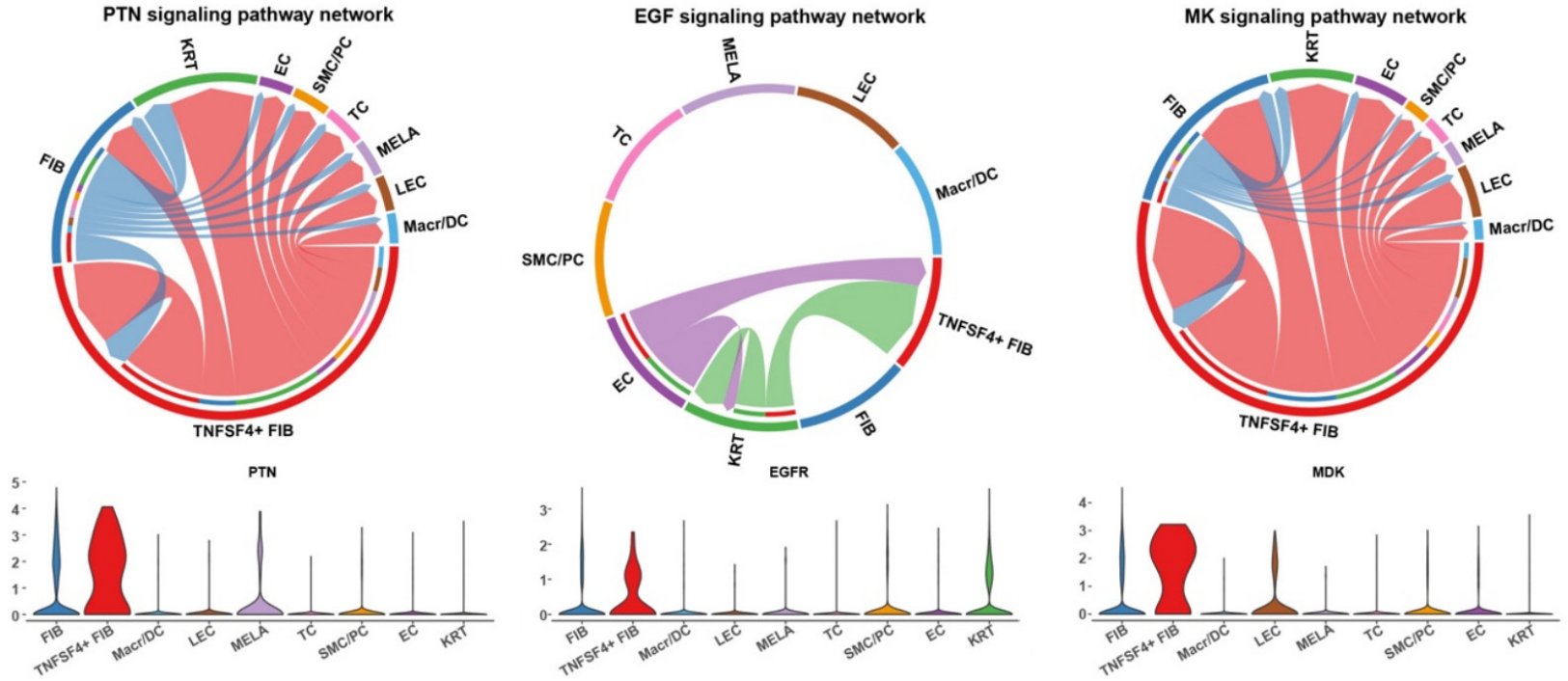
PTN signaling pathway network
KRT
EC
SMC/PC
TC
MELA
LEC
Macr/DC
FIB
TNFSF4+ FIB
EGF signaling pathway network
MELA
LEC
TC
Macr/DC
SMC/PC
TNFSF4+ FIB
EC
FIB
KRT
MK signaling pathway network
KRT
EC
SMC/PC
FIB
TC
MELA
LEC
Macr/DC
TNFSF4+ FIB
PTN
EGFR
MDK
FIB
TNFSF4+ FIB
Macr/DC
LEC
MELA
TC
SMC/PC
EC
KRT

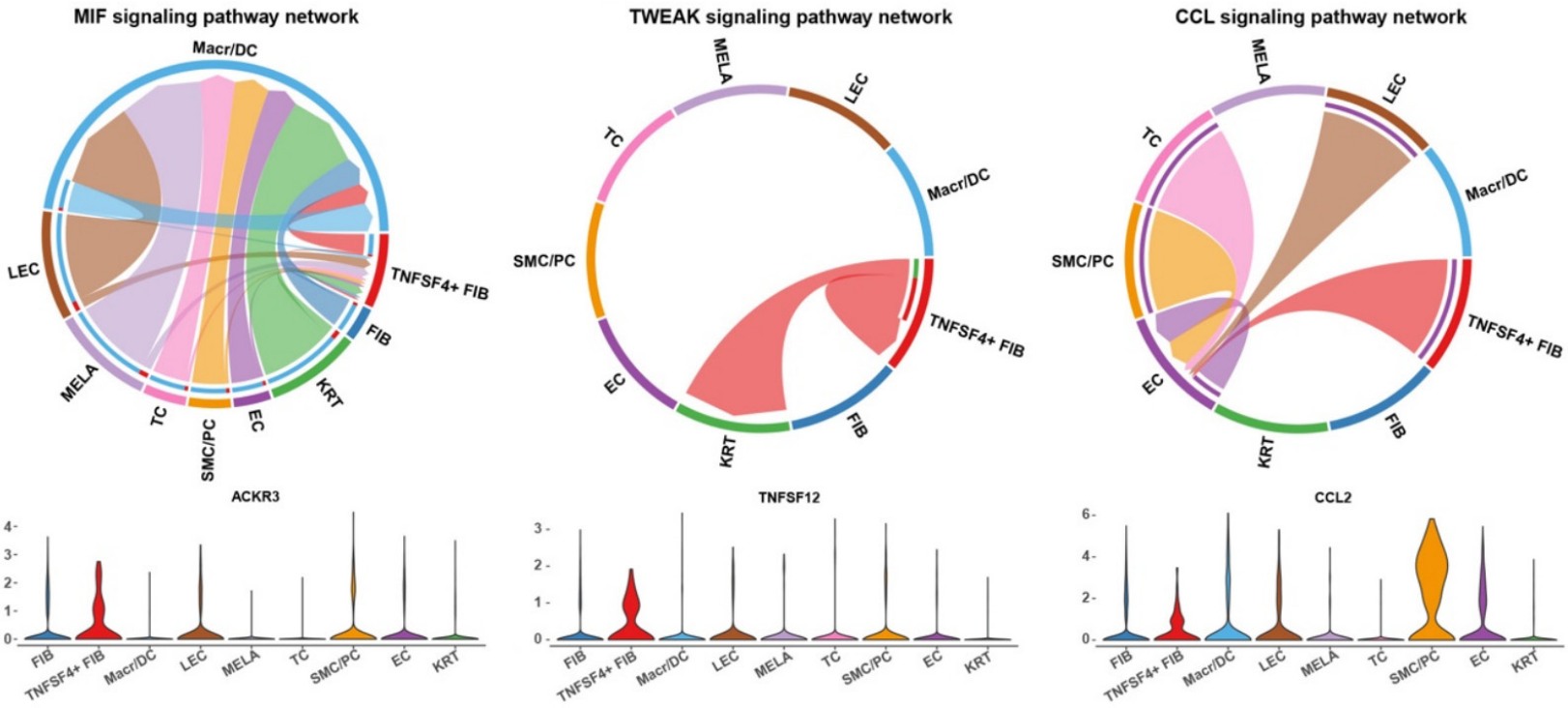

Figure 6. A number of intercellular interactions were greatly altered in TNFSF4+ fibroblasts compared to fibroblasts, involving multiple signaling axes including PTN (pleiotrophin), EGF (epidermal growth factor), MK (midkine), MIF (macrophage migration inhibitory factor), TWEAK (TNF-related weak inducer of apoptosis), and CCL (C-C motif chemokine ligand). The violin diagrams below illustrate the expression of the major ligands or receptors of the signaling pathways in different cell types. FIB, fibroblast; EC, endothelial cell; KRT, keratinocyte; MELA, melanocyte; PC, pericyte; SMC, smooth muscle cell; DC, dendritic cell; TC, T cell; Macr, macrophage.

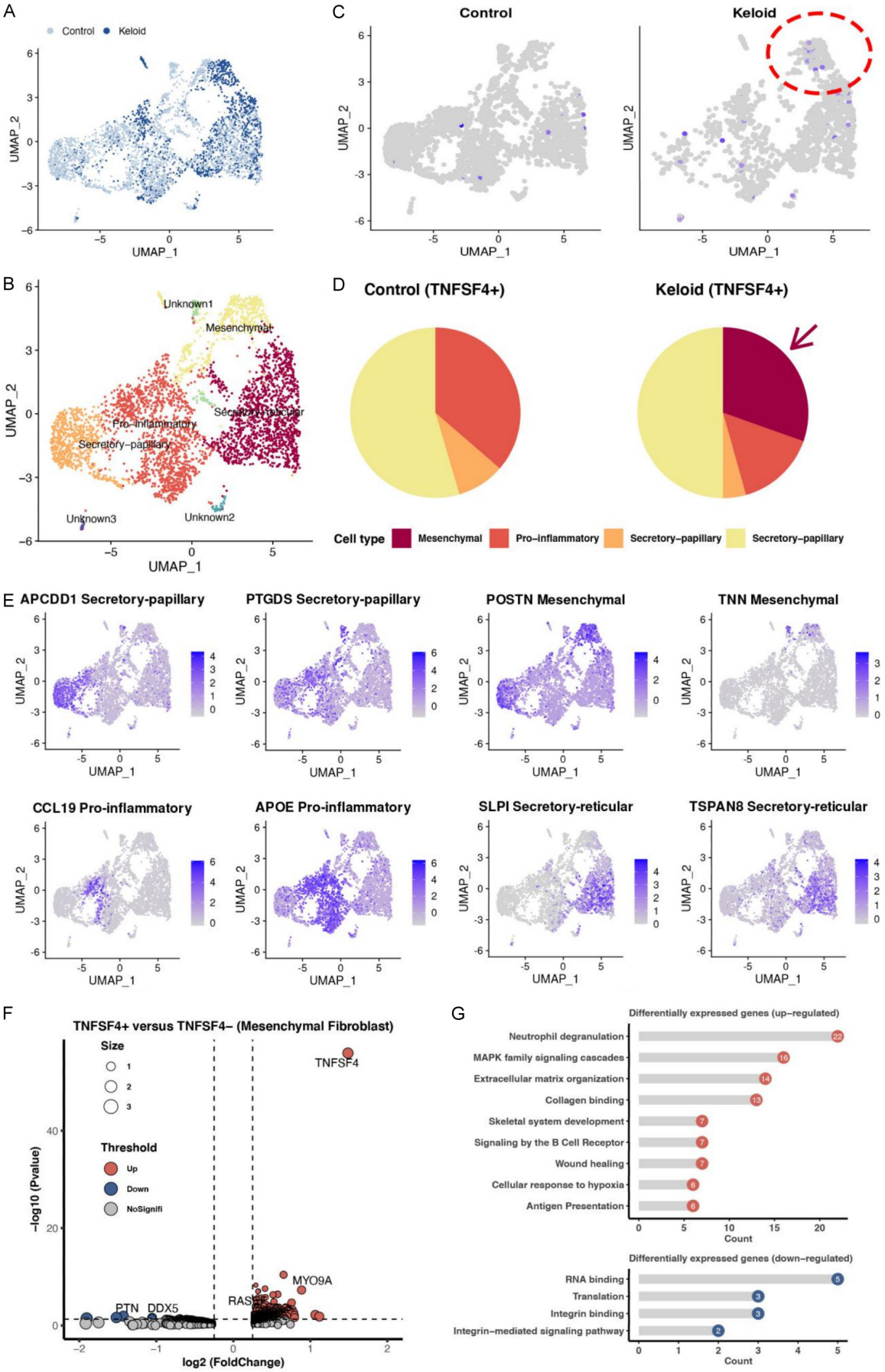
A
Control
Keloid
UMAP_2
UMAP_1
C
Control
Keloid
B
Unknown1
Mesenchymal
Pro−inflammatory
Secretory−papillary
Unknown3
Unknown2
D
Control (TNFSF4+)
Keloid (TNFSF4+)
Cell type
Mesenchymal
Pro−inflammatory
Secretory−papillary
Secretory−papillary
E
APCDD1 Secretory-papillary
PTGDS Secretory-papillary
POSTN Mesenchymal
TNN Mesenchymal
CCL19 Pro-inflammatory
APOE Pro-inflammatory
SLPI Secretory-reticular
TSPAN8 Secretory-reticular
F
TNFSF4+ versus TNFSF4− (Mesenchymal Fibroblast)
Size
Threshold
Up
Down
NoSignifi
TNFSF4
MYO9A
RAS
PTN
DDX5
−log10 (Pvalue)
log2 (FoldChange)
G
Differentially expressed genes (up−regulated)
Neutrophil degranulation
MAPK family signaling cascades
Extracellular matrix organization
Collagen binding
Skeletal system development
Signaling by the B Cell Receptor
Wound healing
Cellular response to hypoxia
Antigen Presentation
Count
Differentially expressed genes (down−regulated)
RNA binding
Translation
Integrin binding
Integrin−mediated signaling pathway
Count

Figure 7. Upregulation of TNFSF4 mainly in mesenchymal fibroblasts. A, B. Subdivision and annotation of fibroblast subtypes. Seven cell clusters were obtained after downscaling of overall fibroblasts. C, D. TNFSF4 expression in fibroblast subpopulations. The red ellipse indicates that the high expression of TNFSF4 is concentrated in the mesenchymal fibroblast cluster. The pie charts show the distribution of cell types expressing TNFSF4 in keloid and control group. E. Expression of representative genes for mesenchymal fibroblasts, pro-inflammatory fibroblasts, secretory papillary fibroblasts and secretory reticular fibroblasts. F. Volcano map of differentially expressed genes in TNFSF4+ mesenchymal fibroblasts compared to TNFSF4- mesenchymal fibroblasts. G. Enrichment analysis of differentially expressed genes in TNFSF4+ mesenchymal fibroblasts.

To the best of our knowledge, there is a paucity of studies and reports on immune molecules in keloids. In this study, we found upregulation of TNFSF4 in keloids using immunogenetic sequencing and GEO datasets. This finding was validated using datasets GSE190626, GSE158395, and GSE178562. Variation in TNFSF4 at the epigenetic level was concordant with expression in the transcriptome; TNFSF4 hypermethylated sites were located in the body region and hypomethylated sites were situated in the TSS200 region of the promoter. Functional enrichment analysis of the protein interaction network constructed based on TNFSF4 indicated that TNFSF4 was involved in multiple immune processes. Single-cell RNA sequencing results suggested that TNFSF4 was highly expressed in MFs, which are pivotal cells in skin fibrosis. This elevated TNFSF4 expression enhanced cell-to-cell interactions in fibrosis-related pathways, such as the FN1 pathway and collagen pathway. TNFSF4-expressing MFs markedly upregulated gene expression in extracellular matrix organization and wound healing processes. Therefore, it is reasonable to conclude that TNFSF4 is a biomolecule that may contribute to the pathogenesis of keloidal scars.

TNFSF4, an immune checkpoint regulator, is a co-stimulatory molecule necessary for full activation of T cells. Its polymorphisms have been linked to a diverse range of immune diseases, such as desiccation syndrome and systemic lupus erythematosus [41-43]. TNFSF4 is a member of the tumor necrosis factor family, which has numerous family members and establishes a complex communication system in various cell types by binding to TNFRSF4, recruiting signal transduction proteins, and activating downstream signaling pathways [44-46]. Single-cell RNA sequencing found that TNFSF4 was highly expressed in MFs. This result suggested that TNFSF4 was an important regulator in the fibrosis process. Elhai et al. found that TNFSF4 protein expression was 3.6-fold higher in systemic sclerosis compared with control samples. They also found positive staining for TNFSF4 in CD90+ and α-smooth muscle actin-positive cells. These results indicate that TNFSF4 is expressed in fibroblasts and myofibroblasts [47]. Furthermore, a fibrogenic model found that TNFSF4 knock-out mice are protected from bleomycin-induced fibrosis and have reduced pro-inflammatory cytokine levels. The abnormal upregulation and function of TNFSF4 in systemic sclerosis are consistent with our keloid lesion results and partially corroborate our findings.

TNFSF4 has been reported to be abnormally upregulated in tumor-associated fibroblasts in stressful environments like chemotherapy and hypoxia. The presence of fibroblasts with increased TNFSF4 expression is correlated with chemoresistance in lung adenocarcinoma [48]. Blockade of immune checkpoints (e.g., TNFSF4/TNFRSF4) targeting immune function stimulation signals is one of the most promising therapeutic tools available for tumors. Programmed death receptors such as TNFRSF4 are expressed on the surface of T cells, while ligands like TNFSF4 are presented on tumor cells. Binding of the receptors to their ligands can appropriately regulate T cell activation [49]. Considering the tumor-like properties of keloids, the development of immunotherapeutic agents targeting a family of immune co-stimulatory molecules may be a promising future direction for keloid treatment.

We found aberrant expression of the immune co-stimulatory molecule TNFSF4 in keloid fibroblasts and its effect on intercellular crosstalk. However, this study had some limitations. First, it was a retrospective study of sequencing data, and the sample size in the keloid dataset was relatively small. Second, there was heterogeneity among patients, especially in the single-cell RNA sequencing results; the generalizability of the results should be confirmed in a large-scale study. Finally, because clinical information for

the patients with keloid lesions was unavailable in several datasets, it was difficult to perform subgroup analysis in terms of age and gender, based on the general profiles of the patients. Considering TNFSF4 has been reported as a biomarker to predict the development of systemic sclerosis, multicenter, large-sample prospective studies are necessary to estimate the predictive power of TNFSF4 for keloids.

Conclusions

This study revealed upregulation of TNFSF4 expression in keloids from an immunological perspective and validated the aberrant expression of TNFSF4 at the methylation and single-cell sequencing levels. The results also suggested upregulation of TNFSF4 expression was specifically clustered in MFs, which is one of the cell types that contributes most during the formation of extracellular matrix in keloids. TNFSF4 may represent a promising new focus for pathogenesis research, and the special status of TNFSF4 as an immune checkpoint molecule may provide a new direction for immunotherapy of keloidal scars.

Acknowledgements

The authors thank the GEO database for providing open-source data and R software for computing support. This study was supported by The National Natural Science Foundation of China (81871538) and Beijing Municipal Commission of Science and Technology (Z191100006619009).

The studies involving human participants were reviewed and approved by Bioethical Committee of Peking Union Medical College Hospital (JS-2907). The patients/participants provided their written informed consent to participate in this study.

Disclosure of conflict of interest

The authors declare that the research was conducted in the absence of any commercial or financial relationships that could be construed as a potential conflict of interest.

Abbreviations

DEGs, Differentially expressed genes; ECM, Extracellular matrix; GEO, Gene Expression Omnibus; GSE, Gene set ensemble; GSM, Gene set matrix; FC, fold change; GO, Gene ontology; GSEA, gene set enrichment analysis; PPI, Protein-protein interaction; TNFSF, Tumor necrosis factor superfamily; TNFRSF, Tumor necrosis factor receptor superfamily; scRNA, Single-cell RNA; TSS, Transcription start site; PCA, Principal component analysis; TSLP, Thymic stromal lymphopoietin.

Address correspondence to: Youbin Wang, Department of Plastic Surgery, Peking Union Medical College Hospital, Beijing, China. E-mail: wybenz@sina.com

References

[1] Barone N, Safran T, Vorstenbosch J, Davison PG, Cugno S and Murphy AM. Current advances in hypertrophic scar and keloid management. Semin Plast Surg 2021; 35: 145-152.
[2] Huang C and Ogawa R. Systemic factors that shape cutaneous pathological scarring. Faseb J 2020; 34: 13171-13184.
[3] Ekstein SF, Wyles SP, Moran SL and Meves A. Keloids: a review of therapeutic management. Int J Dermatol 2021; 60: 661-671.
[4] Andrews JP, Marttala J, Macarak E, Rosenbloom J and Uitto J. Keloids: the paradigm of skin fibrosis - pathomechanisms and treatment. Matrix Biol 2016; 51: 37-46.
[5] Kwon HE, Ahn HJ, Jeong SJ and Shin MK. The increased prevalence of keloids in atopic dermatitis patients with allergic comorbidities: a nationwide retrospective cohort study. Sci Rep 2021; 11: 23669.
[6] Bagabir R, Byers RJ, Chaudhry IH, Müller W, Paus R and Bayat A. Site-specific immunophenotyping of keloid disease demonstrates immune upregulation and the presence of lymphoid aggregates. Br J Dermatol 2012; 167: 1053-1066.
[7] Li Y, Li M, Qu C, Li Y, Tang Z, Zhou Z, Yu Z, Wang X, Xin L and Shi T. The polygenic map of keloid fibroblasts reveals fibrosis-associated gene alterations in inflammation and immune responses. Front Immunol 2021; 12: 810290.
[8] Kolahian S, Fernandez IE, Eickelberg O and Hartl D. Immune mechanisms in pulmonary fibrosis. Am J Respir Cell Mol Biol 2016; 55: 309-322.
[9] Schulz JN, Plomann M, Sengle G, Gullberg D, Krieg T and Eckes B. New developments on skin fibrosis - essential signals emanating from the extracellular matrix for the control of myofibroblasts. Matrix Biol 2018; 68-69: 522-532.
[10] Weiskirchen R, Weiskirchen S and Tacke F. Organ and tissue fibrosis: molecular signals,

cellular mechanisms and translational implications. Mol Aspects Med 2019; 65: 2-15.
[11] Wang CH, Shan MJ, Liu H, Hao Y, Song KX, Wu HW, Meng T, Feng C, Qi Z, Wang Z and Wang YB. Hyperbaric oxygen treatment on keloid tumor immune gene expression. Chin Med J (Engl) 2021; 134: 2205-2213.
[12] Hahn JM, Glaser K, McFarland KL, Aronow BJ, Boyce ST and Supp DM. Keloid-derived keratinocytes exhibit an abnormal gene expression profile consistent with a distinct causal role in keloid pathology. Wound Repair Regen 2013; 21: 530-544.
[13] Fuentes-Duculan J, Bonifacio KM, Suárez-Fariñas M, Kunjravia N, Garcet S, Cruz T, Wang CQF, Xu H, Gilleadeau P, Sullivan-Whalen M, Tirgan MH and Krueger JG. Aberrant connective tissue differentiation towards cartilage and bone underlies human keloids in African Americans. Exp Dermatol 2017; 26: 721-727.
[14] Xie J, Chen L, Cao Y, Wu D, Xiong W, Zhang K, Shi J and Wang M. Single-cell sequencing analysis and weighted co-expression network analysis based on public databases identified that TNC is a novel biomarker for keloid. Front Immunol 2021; 12: 783907.
[15] Wu J, Del Duca E, Espino M, Gontzes A, Cueto I, Zhang N, Estrada YD, Pavel AB, Krueger JG and Guttman-Yassky E. RNA sequencing keloid transcriptome associates keloids with Th2, Th1, Th17/Th22, and JAK3-skewing. Front Immunol 2020; 11: 597741.
[16] Matsumoto NM, Aoki M, Okubo Y, Kuwahara K, Eura S, Dohi T, Akaishi S and Ogawa R. Gene expression profile of isolated dermal vascular endothelial cells in keloids. Front Cell Dev Biol 2020; 8: 658.
[17] Griffin MF, Borrelli MR, Garcia JT, Januszyk M, King M, Lerbs T, Cui L, Moore AL, Shen AH, Mascharak S, Diaz Deleon NM, Adem S, Taylor WL, desJardins-Park HE, Gastou M, Patel RA, Duoto BA, Sokol J, Wei Y, Foster D, Chen K, Wan DC, Gurtner GC, Lorenz HP, Chang HY, Wernig G and Longaker MT. JUN promotes hypertrophic skin scarring via CD36 in preclinical in vitro and in vivo models. Sci Transl Med 2021; 13: eabb3312.
[18] Gautier L, Cope L, Bolstad BM and Irizarry RA. affy--analysis of Affymetrix GeneChip data at the probe level. Bioinformatics 2004; 20: 307-315.
[19] Ritchie ME, Phipson B, Wu D, Hu Y, Law CW, Shi W and Smyth GK. limma powers differential expression analyses for RNA-sequencing and microarray studies. Nucleic Acids Res 2015; 43: e47.
[20] Jones LR, Young W, Divine G, Datta I, Chen KM, Ozog D and Worsham MJ. Genome-wide scan for methylation profiles in keloids. Dis Markers 2015; 2015: 943176.
[21] Tian Y, Morris TJ, Webster AP, Yang Z, Beck S, Feber A and Teschendorff AE. ChAMP: updated methylation analysis pipeline for Illumina BeadChips. Bioinformatics 2017; 33: 3982-3984.
[22] Szklarczyk D, Franceschini A, Wyder S, Forslund K, Heller D, Huerta-Cepas J, Simonovic M, Roth A, Santos A, Tsafou KP, Kuhn M, Bork P, Jensen LJ and von Mering C. STRING v10: protein-protein interaction networks, integrated over the tree of life. Nucleic Acids Res 2015; 43: D447-452.
[23] Szklarczyk D, Santos A, von Mering C, Jensen LJ, Bork P and Kuhn M. STITCH 5: augmenting protein-chemical interaction networks with tissue and affinity data. Nucleic Acids Res 2016; 44: D380-384.
[24] Yu G, Wang LG, Han Y and He QY. clusterProfiler: an R package for comparing biological themes among gene clusters. Omics 2012; 16: 284-287.
[25] Subramanian A, Tamayo P, Mootha VK, Mukherjee S, Ebert BL, Gillette MA, Paulovich A, Pomeroy SL, Golub TR, Lander ES and Mesirov JP. Gene set enrichment analysis: a knowledge-based approach for interpreting genome-wide expression profiles. Proc Natl Acad Sci U S A 2005; 102: 15545-15550.
[26] Direder M, Weiss T, Copic D, Vorstandlechner V, Laggner M, Pfisterer K, Mildner CS, Klas K, Bormann D, Haslik W, Radtke C, Farlik M, Shaw L, Golabi B, Tschachler E, Hoetzenecker K, Ankersmit HJ and Mildner M. Schwann cells contribute to keloid formation. Matrix Biol 2022; 108: 55-76.
[27] Butler A, Hoffman P, Smibert P, Papalexi E and Satija R. Integrating single-cell transcriptomic data across different conditions, technologies, and species. Nat Biotechnol 2018; 36: 411-420.
[28] Jin S, Guerrero-Juarez CF, Zhang L, Chang I, Ramos R, Kuan CH, Myung P, Plikus MV and Nie Q. Inference and analysis of cell-cell communication using CellChat. Nat Commun 2021; 12: 1088.
[29] Arechederra M, Daian F, Yim A, Bazai SK, Richelme S, Dono R, Saurin AJ, Habermann BH and Maina F. Hypermethylation of gene body CpG islands predicts high dosage of functional oncogenes in liver cancer. Nat Commun 2018; 9: 3164.
[30] Chatila K, Ren G, Xia Y, Huebener P, Bujak M and Frangogiannis NG. The role of the thrombospondins in healing myocardial infarcts. Cardiovasc Hematol Agents Med Chem 2007; 5: 21-27.

[31] Filippou PS, Karagiannis GS and Constantinidou A. Midkine (MDK) growth factor: a key player in cancer progression and a promising therapeutic target. Oncogene 2020; 39: 2040-2054.
[32] Yao J, Hu XF, Feng XS and Gao SG. Pleiotrophin promotes perineural invasion in pancreatic cancer. World J Gastroenterol 2013; 19: 6555-6558.
[33] Zhang N and Deuel TF. Pleiotrophin and midkine, a family of mitogenic and angiogenic heparin-binding growth and differentiation factors. Curr Opin Hematol 1999; 6: 44-50.
[34] Deshmane SL, Kremlev S, Amini S and Sawaya BE. Monocyte chemoattractant protein-1 (MCP-1): an overview. J Interferon Cytokine Res 2009; 29: 313-326.
[35] Solé-Boldo L, Raddatz G, Schütz S, Mallm JP, Rippe K, Lonsdorf AS, Rodríguez-Paredes M and Lyko F. Single-cell transcriptomes of the human skin reveal age-related loss of fibroblast priming. Commun Biol 2020; 3: 188.
[36] Deng CC, Hu YF, Zhu DH, Cheng Q, Gu JJ, Feng QL, Zhang LX, Xu YP, Wang D, Rong Z and Yang B. Single-cell RNA-seq reveals fibroblast heterogeneity and increased mesenchymal fibroblasts in human fibrotic skin diseases. Nat Commun 2021; 12: 3709.
[37] Limandjaja GC, Niessen FB, Scheper RJ and Gibbs S. The keloid disorder: heterogeneity, histopathology, mechanisms and models. Front Cell Dev Biol 2020; 8: 360.
[38] O'Brien L and Jones DJ. Silicone gel sheeting for preventing and treating hypertrophic and keloid scars. Cochrane Database Syst Rev 2013; 2013: Cd003826.
[39] Wang ZC, Zhao WY, Cao Y, Liu YQ, Sun Q, Shi P, Cai JQ, Shen XZ and Tan WQ. The roles of inflammation in keloid and hypertrophic scars. Front Immunol 2020; 11: 603187.
[40] Cunninghame Graham DS, Graham RR, Manku H, Wong AK, Whittaker JC, Gaffney PM, Moser KL, Rioux JD, Altshuler D, Behrens TW and Vyse TJ. Polymorphism at the TNF superfamily gene TNFSF4 confers susceptibility to systemic lupus erythematosus. Nat Genet 2008; 40: 83-89.
[41] Manku H, Graham DS and Vyse TJ. Association of the co-stimulator OX40L with systemic lupus erythematosus. J Mol Med (Berl) 2009; 87: 229-234.
[42] Webb GJ, Hirschfield GM and Lane PJ. OX40, OX40L and autoimmunity: a comprehensive review. Clin Rev Allergy Immunol 2016; 50: 312-332.
[43] Mahlios J, De la Herrán-Arita AK and Mignot E. The autoimmune basis of narcolepsy. Curr Opin Neurobiol 2013; 23: 767-773.
[44] Croft M, So T, Duan W and Soroosh P. The significance of OX40 and OX40L to T-cell biology and immune disease. Immunol Rev 2009; 229: 173-191.
[45] Fu N, Xie F, Sun Z and Wang Q. The OX40/OX40L axis regulates T follicular helper cell differentiation: implications for autoimmune diseases. Front Immunol 2021; 12: 670637.
[46] Hori T. Roles of OX40 in the pathogenesis and the control of diseases. Int J Hematol 2006; 83: 17-22.
[47] Elhai M, Avouac J, Hoffmann-Vold AM, Ruzehaji N, Amiar O, Ruiz B, Brahiti H, Ponsoye M, Fréchet M, Burgevin A, Pezet S, Sadoine J, Guilbert T, Nicco C, Akiba H, Heissmeyer V, Subramaniam A, Resnick R, Molberg Ø, Kahan A, Chiocchia G and Allanore Y. OX40L blockade protects against inflammation-driven fibrosis. Proc Natl Acad Sci U S A 2016; 113: E3901-3910.
[48] Li Y, Chen Y, Miao L, Wang Y, Yu M, Yan X, Zhao Q, Cai H, Xiao Y and Huang G. Stress-induced upregulation of TNFSF4 in cancer-associated fibroblast facilitates chemoresistance of lung adenocarcinoma through inhibiting apoptosis of tumor cells. Cancer Lett 2021; 497: 212-220.
[49] Ishii N, Takahashi T, Soroosh P and Sugamura K. OX40-OX40 ligand interaction in T-cell-mediated immunity and immunopathology. Adv Immunol 2010; 105: 63-98.

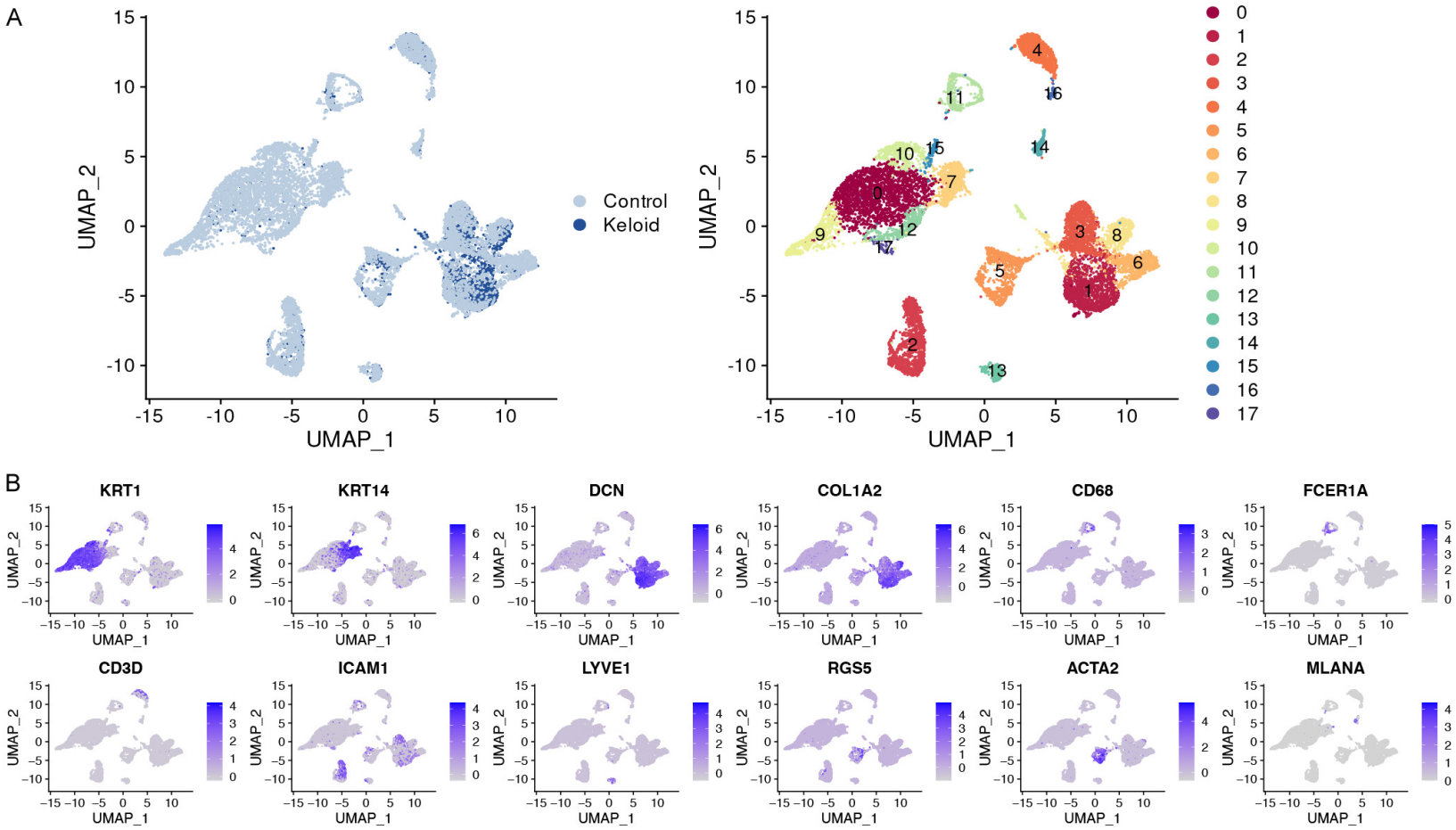

Supplementary Figure 1. A. Descending and clustering analysis. 18 cell clusters were obtained after unsupervised clustering. B. Annotation of cell clusters. Feature plots of the expression of classical cell markers used for cellular annotation.